-RESEARCH PAPER-

International Journal of Mining and Geo-Engineering

IJMGE

IJMGE 60-1 (2026) 57-66

DOI: 10.22059/IJMGE.2025.398485.595277

Gaussian copulas for spatial estimation of ore grade in a copper deposit

Marco Antonio Cotrina-Teatino [a, *], Jairo Jhonatan Marquina-Araujo [a], Jose Nestor Mamani-Quispe [b], Solio Marino Arango-Retamozo [a], Joe Alexis Gonzalez-Vasquez [c], Salomon Ortiz-Quintanilla [d] and Joe Alexis Gonzalez-Vasquez [e]

[a] *Department of Mining Engineering, Faculty of Engineering, National University of Trujillo, Trujillo, Peru.*

[b] *Faculty of Chemical Engineering, National University of the Altiplano, Puno, Peru.*

[c] *Department of Industrial Engineering, National University of Trujillo, Trujillo, Peru.*

[d] *Mining Engineering School, Universidad Nacional Jorge Basadre Grohmann, Tacna, Peru.*

[e] *Department of Metallurgy Engineering, National University of Trujillo, Trujillo, Peru.*

Article History:

Received: 12 July 2025.

Revised: 27 August 2025.

Accepted: 01 November 2025.

ABSTRACT

This study evaluates the effectiveness of the Gaussian copula (GC) in estimating copper grades in a Peruvian copper deposit, comparing its performance with Ordinary Kriging (OK). The methodology was implemented in Python 3.11.7 and Jupyter Notebook 4.2.5. Model accuracy was assessed through 5-fold spatial cross-validation using metrics such as Mean Squared Error (MSE), Mean Bias Error (MBE), Mean Absolute Error (MAE), and Variance. The estimation was conducted using a database of 5,654 composites. The results demonstrate that GC outperforms OK, achieving an MSE of 0.0882, an MAE of 0.1956, an MBE of 0.0394, and a variance of 0.0369. These values indicate that GC provides more accurate and less biased estimates, capturing local grade variability more effectively than OK. Although GC shows slightly higher estimation variance (0.0369 vs. 0.027), it successfully captures the maximum copper grade observed in the real data (2.95%), unlike OK (1.62%), suggesting that GC mitigates the excessive smoothing of OK while still maintaining a centered and stable distribution. In conclusion, the GC method emerges as a robust alternative to OK, offering improved precision, better spatial representation, and enhanced reliability in mineral resource estimation. Its implementation in Python also promotes greater accessibility and reproducibility, reinforcing its value as a practical tool in geostatistics.

Keywords: *Gaussian copulas, Ordinary kriging, Grade estimation, Geostatistics, Spatial dependence.*

1. Introduction

Geostatistics has become a standard methodology for mineral resource estimation and Earth sciences, with Ordinary Kriging (OK) being among the most widely used techniques for spatial interpolation of regionalized variables [1–4]. However, OK presents inherent limitations due to its formulation. Specifically, in ordinary kriging (OK), the weights assigned to sample values depend on the spatial configuration and the covariance model derived from the spatial continuity of the variable [5]. While the weights themselves are independent of the sample magnitudes, the final estimation is a weighted sum of the observed values and therefore incorporates their magnitudes directly. Additionally, OK does not require normally distributed data for estimation [5–9], However, when constructing symmetric confidence intervals based on the Gaussian assumption, a normal transformation is often applied [10]. This transformation facilitates the use of kriging variance to generate confidence intervals, but may introduce bias in skewed datasets.

To overcome these limitations, recent studies have explored the integration of geostatistical models with copulas, particularly Gaussian copulas. Copulas model the joint distribution of random variables with uniform marginals in [0,1] and offer a flexible framework for capturing dependencies [7]. Various types of copulas such as Gaussian, Student's t, chi-square, Gumbel, Clayton, and Frank have been used to represent different dependence structures [11, 12]. In geostatistics, spatial copulas are particularly valuable because they incorporate both the spatial configuration and the value distribution of samples into the estimation process, allowing for more adaptive modeling of spatial variability and the derivation of asymmetric confidence intervals.

The concept of spatial copulas was first introduced by Bárdossy [13] for groundwater quality estimation using Gaussian and chi-square copulas. Due to their relatively simple formulation and ease of implementation, Gaussian copulas have been widely studied in various fields [14, 15]. However, like other elliptical copulas, such as the student's t copula [16], the Gaussian copula has limitations when modeling asymmetric dependence structures, which can lead to an unrealistic representation of spatial variability [13, 17]. To address this, alternative copulas with asymmetric tails, such as the chi-square copula, have been proposed [18]. Nonetheless, copulas remain highly versatile tools in geostatistical applications [19].

In mineral deposit evaluation, grade estimation is based on sparse data from drill holes, which provide only partial information about the deposit [9]. Thus, robust methods are required to infer the spatial distribution of grade values accurately. While OK is commonly used in

* Corresponding author. *E-mail address:* ghadimi@arakut.ac.ir (M. A. Cotrina-Teatino).

the mining industry [20–25]. However, this approach assigns weights to samples exclusively based on their spatial location rather than their grade values [5, 26]. Although ordinary kriging does not require normality for estimation itself, transforming the data into a Gaussian distribution is often recommended when constructing confidence intervals under normality assumptions. This step facilitates the derivation of symmetric confidence bands but may introduce bias in skewed distributions [9]. Alternative methods like Indicator Kriging (IK) attempt to address these shortcomings but may exacerbate the smoothing of extreme values [27, 28].

Gaussian copulas (GC) have been proposed in the literature as an alternative to kriging for estimating variables with spatial dependence, as they enable the simultaneous use of spatial configuration and sample values in weight assignment [13, 29–31]. Similar to IK, Gaussian copulas allow for the derivation of conditional cumulative distributions at unknown locations and the computation of associated confidence intervals [32–35]. However, unlike traditional methods, copulas do not violate ranking order constraints and provide more accurate estimates than ordinary kriging [9].

This study evaluates the application of Gaussian copulas for copper grade estimation in a Peruvian deposit, using open-source tools (Python 3.11.7 and Jupyter Notebook 4.2.5). The proposed algorithm is validated via Jackknife cross-validation and compared with ordinary kriging results [7, 36–38]. Unlike prior works using MATLAB [7–9] or R [39], this implementation in Python improves reproducibility and accessibility. In addition, a set of rigorous statistical metrics is applied to assess model accuracy and bias.

The remainder of the paper is organized as follows: Section 2 details the methodology for spatial estimation using Gaussian copulas; Section 3 presents the case study, validation, and discussion of results; and Section 4 provides the conclusions.

2. Materials and methods

This section presents the theoretical background of GC, which are symmetric functions used to model dependence structures among variables. Although their standard formulation lacks a spatial component, in geostatistics, spatial dependence is introduced via correlograms derived from distance-based analysis, as demonstrated by Bardossy [13, 29], Sohrabian [9], and Atalay [31]. The following subsections describe the implementation of GC estimation in Python, the ordinary kriging method for comparison, and the performance metrics used for model evaluation.

2.1. Gaussian copula

A copula, denoted as C, is a multivariate function that captures the dependence structure among variables, and is defined as:

$$C: [0,1]^n \rightarrow [0,1] \tag{1}$$

If any input variable equals zero, the copula function evaluates to zero, reflecting the boundary behavior of joint distribution functions. According to Sklar's theorem [40], the joint distribution of n variables $F(Z_1, \dots, Z_n)$ can be expressed in terms of their marginal distribution $F_{Z_i}(Z_i)$ and an n-dimensional copula C:

$$C\left(F_{Z_i}(Z_i), \dots, F_{Z_n}(Z_n)\right) = F(Z_1, \dots, Z_n) \tag{2}$$

According to Sklar's theorem, if the marginal distributions are continuous, the copula function C is unique and maps from unit hypercube $[0,1]^n$ to the interval $[0,1]$. This decomposition allows the joint dependence structure to be modeled independently from the marginal distributions, which is particularly advantageous in geostatistics, where spatial dependence and marginal behavior can vary separately.

The copula-based modeling assumes that the involved variables are second-order stationary and share identical marginal distributions across the domain [36]. To apply this approach, continuous variables are first transformed into standard uniform distributions as follows:

$$U_i = F_{Z_i}(Z_i) \tag{3}$$

As a result, the copula function becomes independent of the marginal distributions and fully represents the mutual dependence structure. The inverse transformation gives:

$$F(Z_1, \dots, Z_n) = C(F_{Z_1}^{-1}(Z_1), \dots, F_{Z_n}^{-1}(Z_n)) \tag{4}$$

Here $F_{Z_1}^{-1}(Z_1)$ is the inverse of the marginal distribution of variable i, for $i = 1, \dots, n$.

The copula density function, denoted as c, is computed via partial derivatives:

$$c(u_1, \dots, u_n) = \frac{\partial^n C(u_1,\dots,u_n)}{\partial u_1,\dots,u_n} \tag{5}$$

This density is useful for constructing likelihood functions or simulating data from the copula-based model.

The conditional form of the copula is given by:

This density is useful for constructing likelihood functions or simulating data from the copula-based model.

The conditional form of the copula is given by:

$$C(u_1|U_2 = u_2, \dots, U_n = u_n) = \frac{\frac{\partial^{(n-1)} C(u_1,\dots,u_n)}{\partial u_2,\dots,u_n}}{C(u_2,\dots,u_n)} \tag{6}$$

This conditional form is key for spatial estimation, as it allows the calculation of the distribution at an unsampled location given the observed neighboring values.

In the case of a multivariate Gaussian distribution with correlation matrix R, the Gaussian copula is expressed as:

$$CC_R(Z) = \Phi_R(\Phi^{-1}(Z_1), \dots, \Phi^{-1}(Z_n)) \tag{7}$$

where Φ and Φ^{-1} denote the standard normal CDF and its inverse, respectively. The density of the Gaussian copula, denoted $C_R(.)$, is given by:

$$C_R(Z) = \frac{1}{\sqrt{|R|}} exp\left(-\frac{1}{2}\begin{bmatrix}\Phi^{-1}(Z_1)\\ \dots \\ \Phi^{-1}(Z_n)\end{bmatrix}^T (R^{-1} - I)\begin{bmatrix}\Phi^{-1}(Z_1)\\ \dots \\ \Phi^{-1}(Z_n)\end{bmatrix}\right) \tag{8}$$

Here, $|R|$ is the determinant of the correlation matrix R, I is the identity matrix, and R^{-1} is the inverse of T.

2.2. Spatial copula

Let Z be a second-order stationary variable with marginal distribution F_Z, observed at a set of locations N. Under the assumption of stationarity, the joint exceedance probabilities are invariant under spatial translation:

$$P(Z(x_i) > u_1, \dots, Z(x_k) > u_k) = P(Z(x_i + h) > u_1, \dots, Z(x_k + h) > u_k) \tag{9}$$

where $u_1, \dots, u_k$ are thresholds and h is a lag vector. Based on this, the empirical copula can be expressed as a function of distance:

$$C_s\left(P\left(F_Z > u|Z(x)\right)\right) = C(F_Z\left(Z(x+h)\right) > u|F_Z\left(Z(x)\right) > u) \tag{10}$$

To incorporate spatial structure into the Gaussian copula, empirical autocorrelograms and cross-correlograms are computed. In this study, we use a univariate representation, where the autocorrelogram of Z is fitted to a theoretical model. By applying the modeled correlogram to the distances between sample points and the estimation location, we construct the correlation matrix used to compute the conditional copula density.

Numerical integration and normalization are then applied to obtain the conditional distribution function at each unsampled location. From this, both the expected value and confidence intervals can be derived for a given significance level [13, 29–31].

2.3. Ordinary kriging

Ordinary kriging is a widely used geostatistical technique for

interpolating values at unsampled locations. It is theoretically recognized as the Best Linear Unbiased Estimator (BLUE), minimizing estimation variance under the constraint of unbiasedness, based on a variogram that characterizes spatial continuity [41–45]. In OK, the estimate at a location x_0 is a weighted linear combination of nearby sample values $Z(x_i)$, expressed as:

$$Z^*(x_0) = \sum_{i=1}^{n} \lambda_i Z(x_i) \tag{11}$$

where n is the number of conditioning samples and λ_i are the kriging weights. These weights are determined by solving a linear system that incorporates the spatial covariance structure, typically written in matrix form as:

$$\begin{bmatrix} \gamma_{11} & \cdots & 1 \\ \vdots & \ddots & \vdots \\ 1 & \cdots & 0 \end{bmatrix} \begin{bmatrix} \lambda_1 \\ \vdots \\ -\mu \end{bmatrix} = \begin{bmatrix} \gamma_{10} \\ \vdots \\ 1 \end{bmatrix} \tag{12}$$

Here, γ_{ij} represents the semivariance between locations x_i and x_j, and μ is the Lagrange multiplier ensuring unbiasedness. Although OK does not intrinsically produce confidence intervals, if the estimated variable is assumed to follow a multivariate normal distribution, symmetric confidence intervals can be constructed using:

$$IC_{OK} = Z^*(x_0) \pm \Phi\sigma \tag{13}$$

where σ is the square root of the kriging variance, and Φ is the standard normal deviate corresponding to the chosen confidence level [46].

2.4. Estimation procedure using gaussian copulas

The Gaussian copula-based estimation was implemented through the following steps:

i. Transformation of data to copula space: The copper grade values $Cu\ (x_i)$ were transformed into a standard uniform distribution using the percentile ranking method with the rankdata () function from the SciPy library [9, 47].

ii. Computation and fitting of the correlogram: The empirical correlogram of the transformed variable was computed over discrete distance lags using the Euclidean metric (cdist()). A theoretical model (exponential, logarithmic, or spherical) was then fitted using curve_fit() to estimate the nugget, sill, and range parameters [48, 49].

iii. Selection of optimal conditioning data (NCD): The number of nearest neighbors and optimal search radius were selected based on the fitted correlogram [9].

iv. Conditional copula estimation: To estimate the conditional distribution at an unsampled location, the k nearest neighbors are identified based on spatial distance. A correlation matrix R of size $(k+1)\ x\ (k+1)$ is constructed using the modeled correlogram, where the last row and column represent the estimation location. The matrix is partitioned as:

$R = \begin{bmatrix} R_{11} & R_{12} \\ R_{21} & R_{22} \end{bmatrix}$, where: $R_{11} \in \mathbb{R}^{kxk}$ is the correlation among the k nearest neighbors. $R_{12} \in \mathbb{R}^{kx^1}$ and $R_{21} \in \mathbb{R}^{1xk}$ are the correlations between neighbors and the estimation point. $R_{22} = 1$ is the self-correlation.

Let $Z = (Z_1, Z_2, \ldots, Z_k)$ be the values at the neighbors in copula (Gaussian) space. Then, assuming multivariate normality, the conditional distribution of Z_0 (unsampled point) is:

$$E[Z_0|Z] = R_{21}R_{11}^{-1}Z \tag{14}$$

$$\mathrm{Var}[Z_0|Z] = 1 - R_{21}R_{11}^{-1}R_{12} \tag{15}$$

This conditional normal distribution is transformed to the copula space via the standard normal CDF, and finally, the result is mapped back to the original data space using the inverse of the empirical marginal distribution.

v. For each estimation point, the nearest neighbors were identified based on distance. The transformed values were used to compute the conditional copula density. The resulting distribution was back-transformed using empirical quantiles to yield the final estimates, preserving the original distribution characteristics [9].

Five-fold spatial cross-validation: The model was validated using 5-fold spatial cross-validation, implemented by grouping samples based on spatial proximity to avoid autocorrelation leakage. This procedure was carried out using the KFold() function from Scikit-Learn, and applied identically for both OK and GC methods. The following performance metrics were computed: Mean Squared Error (MSE), Mean Absolute Error (MAE), Mean Bias Error (MBE), and estimation variance [9, 50].

2.5. Evaluation metrics

To evaluate the estimation accuracy, the following metrics were used:

Mean Bias Error: Assesses systematic bias in the estimates. Ideal models exhibit MBE values close to zero [51, 52].

$$MBE = \frac{1}{m}\sum(Cu(x_i) - Cu^*(x_i)) \tag{16}$$

where, $Cu^*(x_i)$ is the estimated copper grade at location x_i and m represents the total number of estimation points.

Mean Squared Error: Quantifies average error magnitude, penalizing large deviations [53, 54]:

$$MSE = \frac{1}{m}\sum(Cu(x_i) - Cu^*(x_i))^2 \tag{17}$$

Variance of estimates: Indicates the smoothing level of the estimator. Higher variance reflects greater dispersion; very low variance may suggest over-smoothing.

$$Var = \frac{1}{m}\sum(Cu(x_i) - Cu^*(x_i)) - MBE)^2 \tag{18}$$

Algorithm 1 Mineral grade estimation using gaussian copulas

Input:

$Cu(x_i)$ sampled copper grades

1. Step1; convert $Cu(x_i)$ to a uniform distribution:
   $U_i = \frac{rank(Cu(x_i))}{n}$
   Store transformation

2. Step2; compute and fit the correlogram:
   Compute the distance matrix $D_{ij} = \|x_i - x_j\|$
   Calculate empirical correlation: $\gamma(h_k) = \frac{1}{2N(h_k)}\sum_{i,j|D_{ij}\approx h_k} (U_i - U_j)^2$
   Fit and exponential model: $\gamma(h) = nugget + sill\ x\ e^{-h/range}$

3. Step3; select optimal neighbors (NCD)
   Determine NCD and R_{opt} based on $\gamma(h)$

4. Step4; estimation with copulas, for each estimation point x_0 do
   Select the NCD nearest neighbors x_j
   Use the modeled correlogram to compute the correlation matrix R
   Partition R into R_{11} (neighbors), R_{12}/R_{21} (cross-correlations), and R_{22} (1)
   Transform U_j to standard normal space:
   Compute:
   $Z_0^* = R_{21}R_{11}^{-1}Z_j$
   $\sigma_0^2 = 1 - R_{21}R_{11}^{-1}R_{12}$
   Back transform:
   $U_0 = \Phi(Z_0)$
   $Cu^*(x_0) = F_{Cu}^{-1}(U_0)$
   Apply inverse transformation:

5. Step5; spatial 5-fold cross-validation and accuracy metrics:
   Group the data into 5 spatially distinct subsets based on

proximity. For each fold, compute $Cu^*(x_i)$.

Mean squared error: $MSE = \frac{1}{m}\sum(Cu(x_i) - Cu^*(x_i))^2$

Mean absolute error: $MAE = \frac{1}{m}\sum|Cu(x_i) - Cu^*(x_i)|$

Mean bias error: $MBE = \frac{1}{m}\sum(Cu(x_i) - Cu^*(x_i))$

Error variance (Var): $Var = \frac{1}{m}\sum(Cu(x_i) - Cu^*(x_i)) - MBE)^2$

end for

end for

6. Step6; comparison

if $MSE_{GC} < MSE_{OK}$ y $|MBE_{GC}| < |MBE_{OK}|$ y $Var_{GC} < Var_{OK}$ then

Accepted estimation with gaussian copula

else

optimize NCD y R_{opt}

end if

output: Estimated copper grade $Cu^*(x_i)$, accuracy metrics (MSE, MAE, MBE, Variance).

3. Results

The deposit under study is a polymetallic mine with a predominant presence of copper (Cu) in Peru, where mineralization is strongly controlled by lithology and associated hydrothermal processes. Five main rock types have been identified in the mineralized zone, each exhibiting specific characteristics that influence the spatial distribution of copper. The Magnetite Skarn (Rock 1) is associated with high copper grades due to intense hydrothermal alteration and metasomatic replacement. Granodiorite (Rock 2), the most represented unit in the database, is an intrusive rock hosting disseminated mineralization. Dacitic Porphyry (Rock 3) contains copper within veinlets and fracture zones. Limestone Sediments (Rock 4) and Catalina Volcanics (Rock 5), though less abundant, may exhibit copper enrichment depending on their interaction with mineralizing fluids [55, 56]. To provide geological context and support this approach, a simplified geological map of the deposit is presented in Figure 1, illustrating the spatial distribution of the main lithologies.

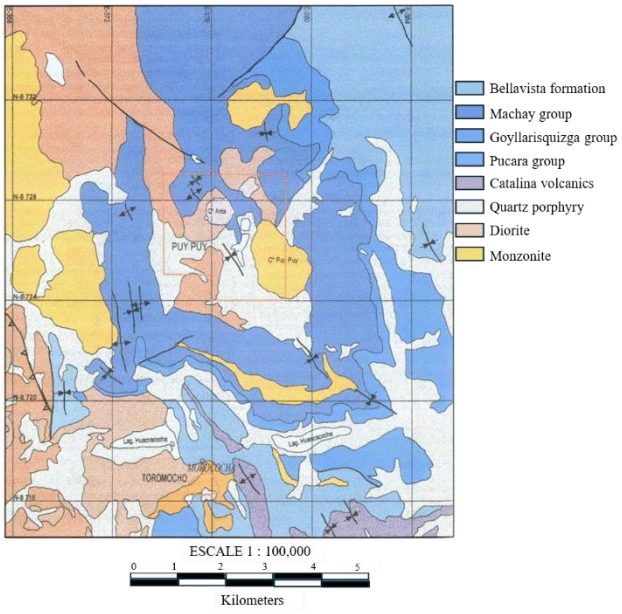

Figure 1. Simplified geological map of the copper deposit, showing the spatial distribution of the main lithological units.

3.1. Data description

The statistical analysis of 5654 composites reflects the spatial heterogeneity of copper mineralization within the mine. The mean copper grade is 0.43%, with values ranging from 0.00% to 2.95%, indicating the presence of high-mineralization zones. The grade distribution exhibits a positive skewness of 1.21 and a kurtosis of 2.73, suggesting the presence of outliers with elevated copper grades, likely concentrated in the Skarn and Dacitic Porphyry zones. The variance of 0.08 and a standard deviation of 0.29 confirm a significant dispersion in copper values, implying the influence of multiple lithologies on mineral distribution (see Table 1). Additionally, lithology was treated as a categorical variable. The most frequently occurring rock type in the database is Granodiorite (Code 2), representing approximately 58.67% of the samples. This suggests that Granodiorite serves as the predominant rock for copper mineralization in the deposit (see Table 2).

Figure 2 illustrates the three-dimensional distribution of drill holes conducted in the mine, representing the variability of copper grade (%) throughout the deposit. A predominant concentration of low to moderate copper values (blue shades) is observed, with localized zones of higher enrichment (green to red shades).

Table 1. Descriptive statistics of the database.

Feature	East (m)	North (m)	Elevation (m)	Copper grade (%)
Count	5654	5654	5654	5654
Mean	375606.25	8717015.68	4473.54	0.43
Std dev	307.24	393.54	169.54	0.29
Minimum	374821.06	8716003.08	4050.35	0.00
25%	375393.42	8716738.40	4340.07	0.23
50%	375602.29	8716995.80	4462.81	0.38
75%	375824.99	8717271.73	4607.49	0.58
Maximum	376414.81	8718153.15	4902.14	2.95
Mode	375388.76	8716581.22	4230.33	0.25
Variance	94394.22	154875.70	28743.49	0.08
Skewness	0.01	0.19	0.07	1.21
Kurtosis	-0.45	-0.23	-0.81	2.73

Table 2. Frequency distribution of lithology types in the database.

Rock type code	Lithology name	Count	Percentage (%)
1	Magnetite skarn	906	16.02
2	Granodiorite	3,317	58.67
3	Dacitic porphyry	1,079	19.08
4	Limestone sediment	307	5.43
5	Catalina volcanics	45	0.80
Total		**5654**	**100.0**

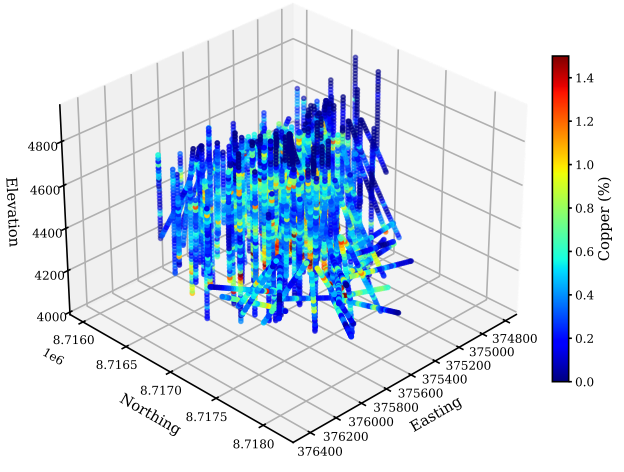

Figure 2. 3D drill holes with copper grade distribution.

3.2. Spatial variability analysis

To ensure reliable copper grade estimations within the deposit, a detailed analysis of spatial variability was conducted. This process involved transforming the original data into both Gaussian and uniform distributions, as well as computing omnidirectional correlograms, which are essential for implementing Gaussian copulas in Python.

Figure 3 illustrates the transformation of copper grade distributions. The left panel displays the Gaussian transformation, which results in a symmetric distribution centered around the mean, ensuring that the data conform to a standard normal distribution. This transformation was necessary for estimation using OK. In contrast, the right panel presents the uniform transformation, where values are evenly distributed within the range [0,1]. These transformations facilitate the modeling of dependence structures independently of the original marginal distribution. The uniform transformation was performed using the rankdata function, while the Gaussian transformation was carried out with SGeMS software [57, 58].

In this study, grade estimation was performed using a single global domain. Although the mineralization is geologically influenced by lithology, an initial structural and exploratory data analysis showed no strong evidence of spatial anisotropy or abrupt grade boundaries that would justify the definition of separate estimation domains. The omnidirectional variogram/correlogram model was selected based on isotropic behavior observed in experimental structures. This approach was adopted to simplify the comparison between OK and GC methods and ensure both estimators were evaluated under identical spatial conditions.

Table 3 presents the spatial structure parameters used in both OK and GC estimation. Although copulas are typically based on correlation structures (correlograms), in this study a consistent approach was applied by fitting both the variogram (used in OK) and the correlogram (used in GC) to the same theoretical model with identical range (81.25 m), ensuring comparable neighborhood influence. For GC, the correlogram was modeled indirectly using the same nugget, sill, and range parameters as the variogram to maintain consistency across methods.

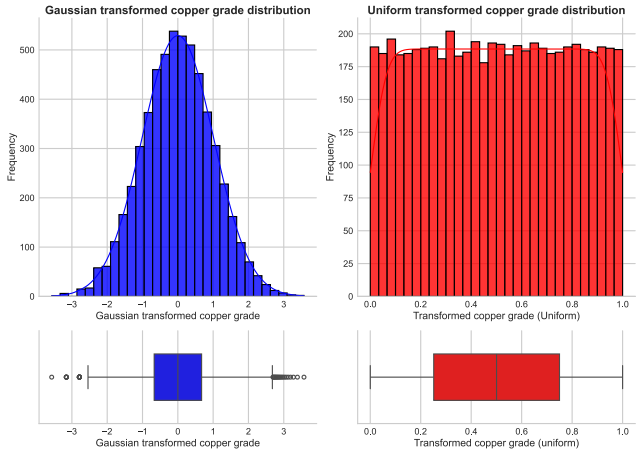

Figure 3. Transformed copper grade distributions.

Table 3. Spatial structure parameters used in ordinary kriging and Gaussian copula estimation.

	Nugget	Sill	Range
Variogram	0.038	0.800	81.25
Correlogram	0.033	0.887	81.25

Figure 3 illustrates the experimental correlogram of the transformed values alongside the fitted model. A strong correlation is observed at short distances, followed by a gradual stabilization, indicating the spatial influence range of the data. This analysis was performed by computing the distance matrix between drill holes and fitting an exponential model using the curve_fit function [59].

The main advantage of the GC method over OK lies in its ability to model complex, non-linear dependencies between spatial data points while preserving the original marginal distribution. Unlike OK, which assumes linear relationships and relies solely on a variogram-based spatial structure, the GC method uses a copula-based joint distribution to capture more flexible spatial interactions. This allows GC to generate conditional cumulative distributions at unsampled locations, enabling both point estimates and the construction of asymmetric confidence intervals. Additionally, the GC method incorporates both the spatial configuration and the sample values into the estimation process, offering better adaptation to local variations and a more accurate representation of spatial heterogeneity. These characteristics make GC particularly useful in deposits with skewed grade distributions or non-stationary behavior.

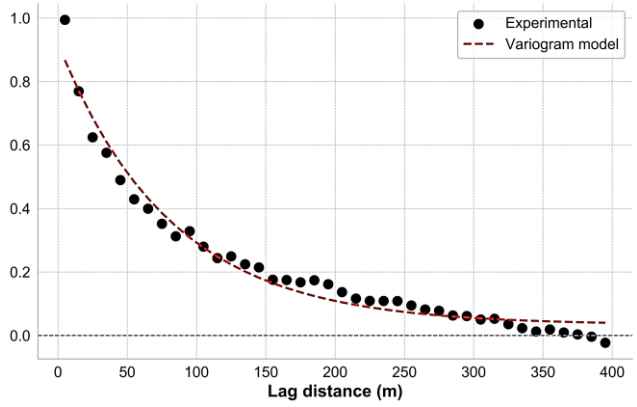

Figure 3. Experimental and fitted correlogram for Gaussian copula estimation.

3.3. Performance evaluation using 5-fold cross-validation

This study evaluates the performance of OK and GC estimation methods through 5-fold spatial cross-validation, aiming to assess the accuracy and bias of copper grade estimations in a copper deposit. For the implementation of the GC method, advanced statistical techniques were applied to model nonlinear dependencies between geospatial variables, which is crucial for accurately representing the structural complexity of mining data. Cross-validation was carried out by selecting 17 nearest neighbors (NCD) for each fold as conditioning data, based on a preliminary cross-validation analysis. The optimal search radius was set to 81.25 meters to maximize estimation accuracy while minimizing the influence of local fluctuations. Both methods, OK and GC, were evaluated under identical conditions, allowing for a direct performance comparison.

Table 4 presents key metrics obtained through 5-fold cross-validation, including MBE, MSE, MAE, and variance for the OK and GC methods. The results indicate that the GC method outperforms OK in terms of estimation accuracy. Specifically, GC achieved a lower MSE (0.0882 vs. 0.126) and MAE (0.1956 vs. 0.264), indicating smaller overall and absolute prediction errors. Although the MBE of GC (0.0394) is slightly farther from zero than OK (-0.006), both values remain close to zero, suggesting that both methods produce nearly unbiased estimates. GC shows a slightly higher estimation variance (0.0369 vs. 0.027); however, it reproduces the actual maximum copper grade (2.95%), unlike OK (1.62%), and its narrower interquartile range suggests more precise estimates. This indicates that GC mitigates the smoothing typically observed in OK, capturing extreme values more effectively while maintaining estimate stability.

Figure 5 presents a boxplot comparing the copper grade distribution of the real dataset against the estimates generated by OK and GC methods. The actual maximum copper grade reaches 2.95%, while the

maximum values estimated by OK and GC are 1.62% and 2.95%, respectively, indicating that only GC successfully reproduces the maximum real value. The median grade from the real data is 0.58%, which is higher than both OK (0.41%) and GC (0.38%). Additionally, the interquartile range of GC is slightly narrower than that of OK, suggesting more concentrated and less dispersed predictions.

Figure 6 shows the variance distribution of copper estimates produced by OK and GC. On average, GC exhibits a slightly higher variance (0.347) compared to OK (0.318). However, the shape of the boxplots shows that OK's estimates have a denser concentration below 0.5 with more compact outliers, whereas GC displays a more concentrated distribution but successfully estimates the real maximum value, which OK fails to reach. This indicates that while GC smooths less than OK in terms of upper extremes, it still maintains a more stable distribution overall.

Figure 7 illustrates the frequency distribution of copper estimates for both OK and GC. Both methods produce positively skewed, unimodal distributions, but GC's curve is noticeably sharper and narrower, centered around ~0.35%. This indicates that GC tends to concentrate its estimations closer to the mean, reflecting a smoother and more conservative estimation behavior. Conversely, OK displays a wider and flatter distribution, showing a greater spread of values, which can result in less stable estimations across the domain.

3.4. Copper grade estimation in the deposit

The copper grade estimation was performed using a block model within a 3D grid. Each block had dimensions of 30 m × 30 m × 30 m, resulting in a total of 112,570 blocks. The Gaussian copula parameters obtained from the Jackknife validation test were incorporated into the estimation process.

Figure 8 compares the copper grade distributions estimated using OK (left) and GC (right) at a constant elevation of Y = 8716600. The OK estimation produces a smoother distribution, where high-grade areas appear more dispersed and less concentrated. In contrast, the GC estimation exhibits a more localized distribution, with well-defined high-grade copper zones and sharper transitions between high- and low-grade areas. This behavior reflects the greater variability and sensitivity of the GC method in capturing local structures.

Figure 9 provides a 3D visualization of the spatial distributions of estimated copper grades using OK and GC at different deposit elevations.

Table 4. Performance metrics for estimation models (OK vs. GC, 5-fold cross-validation).

Metric	Ordinary kriging (OK)	Gaussian copula (GC, mean of 5 folds)
MSE	0.126	0.0882
MAE	0.264	0.1956
MBE	-0.006	0.0394
Variance	0.027	0.0369

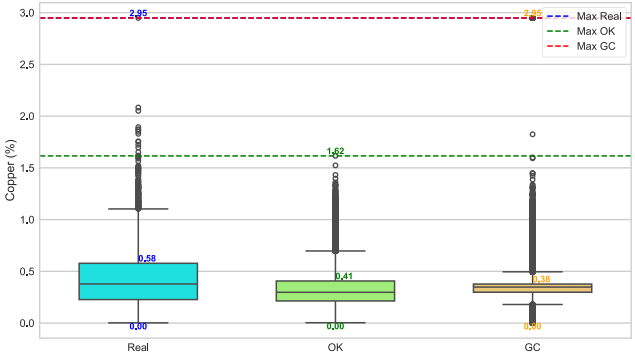

Figure 1. Box plot comparing copper grade estimates from OK and GC methods.

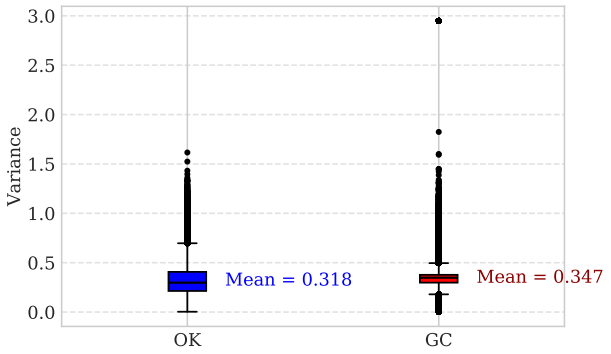

Figure 6. Comparison of variance in copper grade estimation using OK and GC.

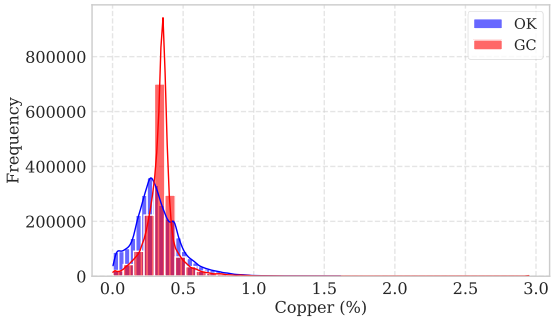

Figure 7. Frequency distribution of estimated copper grades using OK and GC.

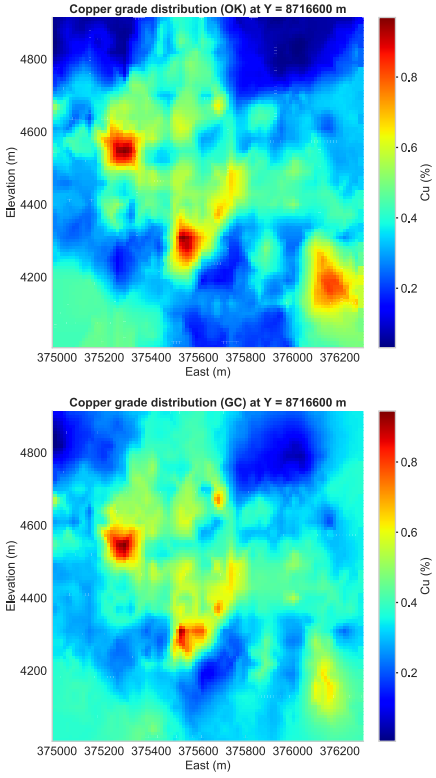

Figure 8. Comparison of copper grade estimates using OK and GC at Y=8716600.

Figure 10 shows the grade-tonnage response curves for OK and GC, based on the same block model and consistent estimation parameters. The curves indicate that GC predicts higher tonnages at lower cut-offs,

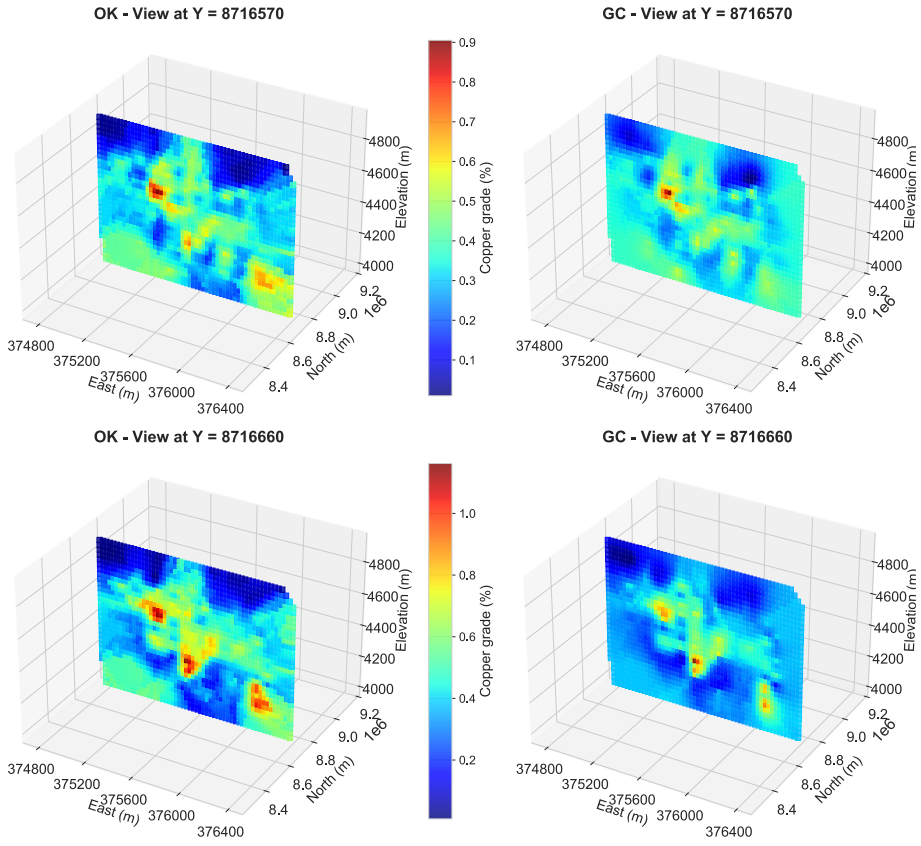

Figure 9. 3D visualization of copper grade estimates using ordinary kriging and gaussian copulas.

while OK surpasses GC at higher thresholds. The average copper grade increases with the cut-off in both methods; however, GC consistently yields higher values, demonstrating its ability to preserve high-grade zones. These results are consistent with the findings of Atalay et al. [31], reinforcing the idea that GC produces more selective estimates, particularly at elevated cut-offs.

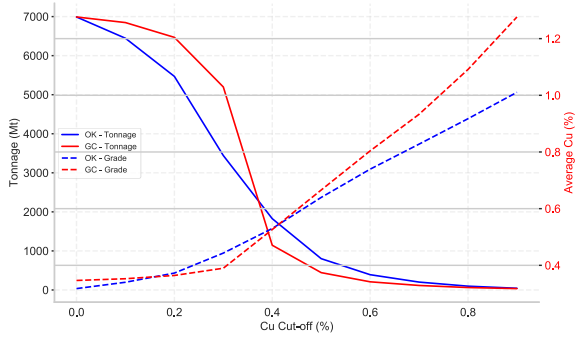

Figure 2. Tonnage and average copper grade as a function of Cu cut-off for OK and GC.

This study evaluates two main approaches for copper grade estimation: OK and GC, comparing their performance through various accuracy metrics. The results suggest that GC provides a more accurate and less biased alternative to OK, aligning with previous studies that have also highlighted the effectiveness of copulas in geostatistical estimation. The MSE for GC estimation in this study was 0.0882, which is slightly higher than the 0.084 reported by Sohrabian and Tercan [9] but significantly lower than the 0.149 found by Sohrabian et al [7]. This reflects a strong level of accuracy, further enhanced by the Python implementation and the use of 5-fold cross-validation, which increased model robustness compared to other methodologies.

The MAE obtained for the GC model was 0.1956. While this metric is not commonly reported in similar studies, its relatively low value suggests competitive performance in estimating copper grades. Sohrabian et al. [7], who tested several copula families on a porphyry copper deposit in Iran, found Gumbel, Frank, and Clayton copulas to be effective, though MAE values were not explicitly discussed. Their results, however, support the use of copulas to model spatial variability an outcome that aligns with the findings of this work.

In terms of MBE, this study achieved a value of 0.0394, indicating a slight positive bias. This is notably lower in magnitude than the negative biases reported by Sohrabian and Tercan [9] (−0.089) and Sohrabian et al. [7] (−0.124), suggesting that the GC-based estimates in this study are more centered and balanced. These results are consistent with the work of Atalay et al. [31], who noted that GC typically produce globally unbiased estimates, with the ability to capture sharp transitions in mineral grade distributions. Unlike the findings of Bárdossy [13], where GC were rejected for certain hydrogeological applications, this study confirms their effectiveness in modeling copper grades likely due to the spatial complexity and variability of the studied deposit. Furthermore, the improved results obtained here reinforce the conclusion of Sohrabian et al. [7] that copula-based methods whether Gaussian or alternative families can outperform kriging under appropriate spatial configurations.

In terms of variance, the GC model in this study achieved a value of 0.0369, which is higher than the 0.027 reported by Sohrabian et al. [9] but still lower than the 0.050 observed by Sohrabian et al. [7]. This intermediate result suggests a balance between capturing spatial variability and maintaining estimate stability. The implementation of the GC in Python, combined with 5-fold cross-validation, likely contributed to enhanced estimator performance, yielding reliable copper grade predictions for the studied Peruvian deposit.

Furthermore, these findings align with the observations of Atalay et al. [31], who highlighted that GC generate higher tonnage and greater mean grades at elevated cut-offs, whereas at lower cut-offs, they yield lower tonnage estimates, reflecting greater precision in mineral resource estimation. This is consistent with the present study, which also demonstrates an improved ability to adapt estimations to the spatial distribution of copper grades. A key contribution of this study is the implementation of GC in Python, representing a significant improvement over previous studies that utilized MATLAB [7–9] or R [39]. Python not only enhances accessibility and reproducibility but also facilitates rigorous statistical testing, including 5-fold cross-validation, thereby increasing the reliability of the obtained results [60, 61]. This optimization of GC implementation represents a notable advancement in geostatistical estimation methods (see Table 5).

Table 5. Comparative analysis of copula-based estimation metrics.

Metric	This study	Sohrabian and Tercan [9]		Sohrabian et al. [7]	Atalay et al. [31]
MSE	0.0882	0.084	0.149	-	-
MAE	0.1956	-	-	-	-
MBE	0.0394	-0.089	-0.124	-	-
Variance	0.0369	0.027	0.050	0.019	89,434

4. Conclusions

This study evaluated the application of GC for copper grade estimation in a copper deposit in Peru, using a Python-developed algorithm and comparing its performance with OK through 5-fold spatial cross-validation. The results demonstrate that GC outperforms OK in terms of accuracy and bias, achieving a lower MSE = 0.0882, a reduced MAE = 0.1956, and a MBE = 0.0394, which is closer to zero compared to OK (MSE = 0.126, MAE = 0.264, MBE = -0.006). In terms of estimation variance, GC yielded a value of 0.0369, slightly higher than OK (0.027). However, GC accurately captures the maximum copper grade observed in the real data (2.95%), which OK fails to reach. This indicates that GC reduces the smoothing effect associated with OK, providing estimates that are both stable and capable of reflecting local extremes. These outcomes confirm that the GC method better captures the spatial structure and grade distribution of the deposit. Furthermore, the implementation in Python based on correlogram analysis and optimal neighbor selection enabled more realistic spatial interpolation. Its open-source nature also enhances reproducibility and accessibility, representing a valuable contribution to applied geostatistics in the mining industry.

Despite the positive results obtained, this research has some limitations that could be addressed in future studies. First, the implemented model is based on a univariate Gaussian copula applied spatially, meaning that it does not consider multivariate dependency structures with other geological or mineralogical variables. Future research should explore multivariate copulas, which could improve modeling capabilities by incorporating relationships with other geochemical elements or structural attributes of the deposit. Additionally, the model used in this study does not incorporate directional anisotropy or lithological boundaries. Although the current study relied on a global domain supported by isotropic behavior in the experimental correlograms, future work should test estimation within lithological domains and use anisotropic structures to further enhance local accuracy. Finally, although 5-fold cross-validation has provided a robust evaluation of the method, future studies could validate this methodology in different mineral deposits to assess its applicability in various geological settings and enhance its generalization potential.

References

[1]. Sohrabian, B., & Tercan, A. E. (2014). Introducing minimum spatial cross-correlation kriging as a new estimation method of heavy metal contents in soils. Geoderma. doi:https://doi.org/10.1016/j.geoderma.2014.02.014.

[2]. Sohrabian, B., Ozcelik, Y., & Hasanpour, R. (2017). Estimating major elemental oxides of an andesite quarry using compositional kriging. International Journal of Mining, Reclamation and Environment. doi:https://doi.org/10.1080/17480930.2016.1168019.

[3]. Jeuken, R., Xu, C., & Dowd, P. (2020). Improving coal quality estimations with geostatistics and geophysical logs. Natural Resources Research. doi:https://doi.org/10.1007/s11053-019-09609-y.

[4]. Rahimi, H., Asghari, O., & Afshar, A. (2018). A geostatistical investigation of 3D magnetic inversion results using multi-Gaussian kriging and sequential Gaussian co-simulation. Journal of Applied Geophysics. doi:https://doi.org/10.1016/j.jappgeo.2018.05.003.

[5]. Lloyd, C. D., & Atkinson, P. M. (2001). Assessing uncertainty in estimates with ordinary and indicator kriging. Computers & Geosciences. doi:https://doi.org/10.1016/S0098-3004(00)00132-1.

[6]. Gräler, B., & Pebesma, E. (2011). The pair-copula construction for spatial data: A new approach to model spatial dependency. Procedia Environmental Sciences. doi:https://doi.org/10.1016/j.proenv.2011.07.036.

[7]. Sohrabian, B., Soltani-Mohammadi, S., Pourmirzaee, R., & Carranza, E. J. M. (2023). Geostatistical evaluation of a porphyry copper deposit using copulas. Minerals, 13(6), Article 732. doi:https://doi.org/10.3390/min13060732.

[8]. Sohrabian, B., & Tercan, A. E. (2024). Copula-based data-driven multiple-point simulation method. Spatial Statistics, 58, 100802. doi:https://doi.org/10.1016/j.spasta.2023.100802.

[9]. Sohrabian, B., & Tercan, A. (2025). Grade estimation through the Gaussian copulas: A case study. Journal of Mining and Environment, 16, 1–13.

[10]. Gräler, B. (2014). Modelling skewed spatial random fields through the spatial vine copula. Spatial Statistics, 8, 1–14. doi:https://doi.org/10.1016/j.spasta.2014.01.001.

[11]. Shaked, M., & Joe, H. (1998). Multivariate models and dependence concepts. Journal of the American Statistical Association. doi:https://doi.org/10.2307/2669872.

[12]. Frahm, G., Junker, M., & Szimayer, A. (2003). Elliptical copulas: Applicability and limitations. Statistics & Probability Letters. doi:https://doi.org/10.1016/S0167-7152(03)00092-0.

[13]. Bárdossy, A. (2006). Copula-based geostatistical models for groundwater quality parameters. Water Resources Research. doi:https://doi.org/10.1029/2005WR004754.

[14]. Van de Vyver, H., & Van den Bergh, J. (2018). The Gaussian copula model for the joint deficit index for droughts. Journal of Hydrology. doi:https://doi.org/10.1016/j.jhydrol.2018.03.064.

[15]. Li, F., Zhou, J., & Liu, C. (2018). Statistical modelling of extreme storms using copulas: A comparison study. Coastal Engineering. doi:https://doi.org/10.1016/j.coastaleng.2018.09.007.

[16]. Lourme, A., & Maurer, F. (2017). Testing the Gaussian and Student's t copulas in a risk management framework. Economic Modelling. doi:https://doi.org/10.1016/j.econmod.2016.12.014.

[17]. Marchant, B. P., Saby, N. P. A., Jolivet, C. C., Arrouays, D., & Lark, R. M. (2011). Spatial prediction of soil properties with copulas. Geoderma. doi:https://doi.org/10.1016/j.geoderma.2011.03.005.

[18]. Quessy, J. F., Rivest, L. P., & Toupin, M. H. (2019). Goodness-of-fit tests for the family of multivariate chi-square copulas. Computational Statistics & Data Analysis.

doi:https://doi.org/10.1016/j.csda.2019.04.008.

[19]. Musafer, G. N., Thompson, M. H., Wolff, R. C., & Kozan, E. (2017). Nonlinear multivariate spatial modeling using NLPCA and pair-copulas. Geographical Analysis. doi:https://doi.org/10.1111/gean.12126.

[20]. Pardo-Igúzquiza, E., & Dowd, P. A. (2005). EMLK2D: A computer program for spatial estimation using empirical maximum likelihood kriging. Computers & Geosciences. doi:https://doi.org/10.1016/j.cageo.2004.09.020.

[21]. Heriawan, M. N., & Koike, K. (2008). Uncertainty assessment of coal tonnage by spatial modeling of seam distribution and coal quality. International Journal of Coal Geology. doi:https://doi.org/10.1016/j.coal.2008.07.014.

[22]. Vargas-Guzmán, J. A. (2008). Unbiased resource evaluations with kriging and stochastic models of heterogeneous rock properties. Natural Resources Research. doi:https://doi.org/10.1007/s11053-008-9082-9

[23]. Ali Akbar, D. (2012). Reserve estimation of central part of Choghart north anomaly iron ore deposit through ordinary kriging method. International Journal of Mining Science and Technology. doi:https://doi.org/10.1016/j.ijmst.2012.01.022.

[24]. Rohma, N. N. (2022). Estimation of ordinary kriging method with jackknife technique on rainfall data in Malang Raya. International Journal on Information and Communication Technology (IJoICT). doi:https://doi.org/10.21108/ijoict.v8i2.678.

[25]. Lamamra, A., Neguritsa, D. L., & Mazari, M. (2019). Geostatistical modeling by the ordinary kriging in the estimation of mineral resources on the Kieselguhr mine, Algeria. IOP Conference Series: Earth and Environmental Science, 362(1), 012051. doi:https://doi.org/10.1088/1755-1315/362/1/012051.

[26]. Da Rocha, M. M., & Yamamoto, J. K. (2000). Comparison between kriging variance and interpolation variance as uncertainty measurements in the Capanema iron mine, State of Minas Gerais-Brazil. Natural Resources Research. doi:https://doi.org/10.1023/a:1010195701968.

[27]. Fogg, G. E. (1996). Transition probability-based indicator geostatistics. Mathematical Geology. doi:https://doi.org/10.1007/bf02083656.

[28]. Carr, J. R., & Mao, N. (1993). A general form of probability kriging for estimation of the indicator and uniform transforms. Mathematical Geology. doi:https://doi.org/10.1007/BF00894777.

[29]. Bárdossy, A., & Li, J. (2008). Geostatistical interpolation using copulas. Water Resources Research. doi:https://doi.org/10.1029/2007WR006115.

[30]. Kazianka, H., & Pilz, J. (2010). Copula-based geostatistical modeling of continuous and discrete data including covariates. Stochastic Environmental Research and Risk Assessment. doi:https://doi.org/10.1007/s00477-009-0353-8.

[31]. Atalay, F., & Tercan, A. E. (2017). Coal resource estimation using Gaussian copula. International Journal of Coal Geology. doi:https://doi.org/10.1016/j.coal.2017.03.010.

[32]. Käärik, E., & Käärik, M. (2009). Modeling dropouts by conditional distribution, a copula-based approach. Journal of Statistical Planning and Inference. doi:https://doi.org/10.1016/j.jspi.2009.05.020.

[33]. Klugman, S. A. (2011). Copula regression. Variance, 5.

[34]. Kwak, M. (2017). Estimation and inference on the joint conditional distribution for bivariate longitudinal data using Gaussian copula. Journal of the Korean Statistical Society. doi:https://doi.org/10.1016/j.jkss.2016.11.005.

[35]. Chang, B., & Joe, H. (2019). Prediction based on conditional distributions of vine copulas. Computational Statistics & Data Analysis. doi:https://doi.org/10.1016/j.csda.2019.04.015.

[36]. Addo, E., Chanda, E. K., & Metcalfe, A. V. (2017). Estimation of direction of increase of gold mineralisation using pair-copulas. Proceedings of the 22nd International Congress on Modelling and Simulation (MODSIM 2017). doi:https://doi.org/10.36334/modsim.2017.a2.addo.

[37]. Musafer, G. N., Thompson, M. H., Kozan, E., & Wolff, R. C. (2017). Spatial pair-copula modeling of grade in ore bodies: A case study. Natural Resources Research. doi:https://doi.org/10.1007/s11053-016-9314-3.

[38]. Bárdossy, A., & Hörning, S. (2023). Definition of spatial copula based dependence using a family of non-Gaussian spatial random fields. Water Resources Research. doi:https://doi.org/10.1029/2023WR034446.

[39]. Agarwal, G., Sun, Y., & Wang, H. J. (2021). Copula-based multiple indicator kriging for non-Gaussian random fields. Spatial Statistics. doi:https://doi.org/10.1016/j.spasta.2021.100524.

[40]. Sklar, A. (1959). Fonctions de répartition à n dimensions et leurs marges (Distribution functions of n dimensions and their marginals). Publications de l'Institut Statistique de l'Université de Paris, 8.

[41]. Hohn, M. E. (1991). An introduction to applied geostatistics. Computers & Geosciences. doi:https://doi.org/10.1016/0098-3004(91)90055-i.

[42]. Deutsch, C. V. (1996). Correcting for negative weights in ordinary kriging. Computers & Geosciences. doi:https://doi.org/10.1016/0098-3004(96)00005-2.

[43]. Pesquer, L., Cortés, A., & Pons, X. (2011). Parallel ordinary kriging interpolation incorporating automatic variogram fitting. Computers & Geosciences. doi:https://doi.org/10.1016/j.cageo.2010.10.010.

[44]. Munyati, C., & Sinthumule, N. I. (2021). Comparative suitability of ordinary kriging and inverse distance weighted interpolation for indicating intactness gradients on threatened savannah woodland and forest stands. Environmental and Sustainability Indicators. doi:https://doi.org/10.1016/j.indic.2021.100151.

[45]. Daya, A. A., & Bejari, H. (2015). A comparative study between simple kriging and ordinary kriging for estimating and modeling the Cu concentration in Chehlkureh deposit, SE Iran. Arabian Journal of Geosciences. doi:https://doi.org/10.1007/s12517-014-1618-1.

[46]. Paoli, J. N., Tisseyre, B., Strauss, O., & Roger, J. M. (2024). Methods to define confidence intervals for kriged values: Application to precision viticulture data. Precision Agriculture. doi:https://doi.org/10.3920/9789086865147_079.

[47]. Virtanen, P., Gommers, R., Oliphant, T. E., et al. (2020). SciPy 1.0: Fundamental algorithms for scientific computing in Python. Nature Methods. doi:https://doi.org/10.1038/s41592-019-0686-2.

[48]. Abraj, M., Wang, Y. G., & Thompson, M. H. (2022). A new mixture copula model for spatially correlated multiple variables with an environmental application. Scientific Reports. doi:https://doi.org/10.1038/s41598-022-18007-z.

[49]. Bevilacqua, M., Alvarado, E., & Caamaño-Carrillo, C. (2024). A flexible Clayton-like spatial copula with application to bounded support data. Journal of Multivariate Analysis. doi:https://doi.org/10.1016/j.jmva.2023.105277.

[50]. Cristianini, N. (2004). Cross-validation (K-fold cross-validation, leave-one-out, jackknife, bootstrap). Dictionary of Bioinformatics and Computational Biology. doi:https://doi.org/10.1002/9780471650126.dob0148.pub2.

[51]. Jandaghian, Z., & Berardi, U. (2021). The coupling of the Weather Research and Forecasting model with the Urban Canopy Models for climate simulations. In Urban Microclimate Modelling for Comfort and Energy Studies. doi:https://doi.org/10.1007/978-3-030-65421-4_11.

[52]. Kazianka, H., & Pilz, J. (2011). Bayesian spatial modeling and interpolation using copulas. Computers & Geosciences. doi:https://doi.org/10.1016/j.cageo.2010.06.005.

[53]. Hodson, T. O., Over, T. M., & Foks, S. S. (2021). Mean squared error, deconstructed. Journal of Advances in Modeling Earth Systems. doi:https://doi.org/10.1029/2021MS002681.

[54]. Cotrina, M., Marquina, J., Noriega, E., Mamani, J., Ccatamayo, J., Gonzalez, J., & Arango, S. (2024). Predicting open pit mine production using machine learning techniques: A case study in Peru. Journal of Mining and Environment, 15, 1345–1355.

[55]. Marquina, J., Cotrina, M., Mamani, J., Noriega, E., & Vega, J., Cruz, J. (2024). Copper ore grade prediction using machine learning techniques in a copper deposit. Journal of Mining and Environment, 15, 1011–1027.

[56]. Marquina-Araujo, J. J., Cotrina-Teatino, M. A., Cruz-Galvez, J. A., Noriega-Vidal, E. M., & Vega-Gonzalez, J. A. (2024). Application of autoencoders neural network and K-means clustering for the definition of geostatistical estimation domains. Mathematical Modelling of Engineering Problems, 11, 1207–1218.

[57]. Zhang, M., Zhang, Y., & Yu, G. (2017). Applied geostatistics analysis for reservoir characterization based on the SGeMS (Stanford Geostatistical Modeling Software). Open Journal of Yangtze Oil and Gas. doi:https://doi.org/10.4236/ojogas.2017.21004.

[58]. Marwanza, I., Nas, C., Azizi, M. A., & Simamora, J. H. (2019). Comparison between moving windows statistical method and kriging method in coal resource estimation. Journal of Physics: Conference Series, 1402(3), 033016. doi:https://doi.org/10.1088/1742-6596/1402/3/033016

[59]. Lemenkova, P. (2019). Computing and plotting correlograms by Python and R libraries for correlation analysis of the environmental data in marine geomorphology. Journal of Geomorphological Researches, 1.

[60]. Cotrina-Teatino, M. A., Marquina-Araujo, J. J., & Riquelme, Á. I. (2025). Comparison of machine learning techniques for mineral resource categorization in a copper deposit in Peru. Natural Resources Research. doi:https://doi.org/10.1007/s11053-025-10505-x.

[61]. Cotrina-Teatino, M. A., Riquelme, Á. I., Marquina-Araujo, J. J., Mamani-Quispe, J. N., Arango-Retamozo, S. M., Ccatamayo-Barrios, J. H., Donaires-Flores, T., Calla-Huayapa, M. A., & Gonzalez-Vasquez, J. A. (2025). KMeans-Riemannian model for classification of mineral resources in a copper deposit in Peru. International Journal of Mining, Reclamation and Environment. doi:https://doi.org/10.1080/17480930.2025.2518987.